

**LARGE RESONANCE ENHANCED SECOND ORDER SUSCEPTIBILITIES IN
ALKALI HALIDE CRYSTALS DUE TO F_A COLOR CENTERS****M.H. Majlesara¹***Photonics Lab. Dept. of Physics, Teacher Training University,
49 Mofateh Ave. 15414 Tehran, Iran*

Received 2 August 2005, in final form 25 April 2006, accepted 10 May 2006

Model calculation of second order susceptibilities for F_A color centers in wide band gap materials is reported. The second order optical nonlinearity in KCl:Li crystals due to F_A color centers evaluated theoretically. The density matrix formalism is employed and the equation of motion is solved by second order perturbation to evaluate the nonlinear optical susceptibility for second harmonic generation as well as frequency mixing. It is found that the system shows large resonance-enhanced second order susceptibilities ($\sim 10^{-16} mV^{-1}$) for color center concentration of $\sim 10^{23} m^{-3}$. A scheme of phase matching in terms of anomalous dispersion of the centers and coherent length are discussed.

PACS: 42.65. An; 42.65.Ky; 42.79.Nv

1. Introduction

Though research work spanning almost two centuries had laid out the foundation of linear optical thoroughly, it is the discovery of powerful optical sources such as lasers that caused rapid developments in the newly established area of nonlinear optics second harmonic generation is the first nonlinear optical effect ever observed in which a coherent input generates a coherent output. But nonlinear optics covers a much broader scope. It deals in general with nonlinear interaction of light with matter and includes such problems as light-induced changes of the optical properties of a medium. Second harmonics generation is then not the first nonlinear optical effect over observed. Optical pumping is certainly a nonlinear optical phenomenon well known before the advent of lasers. Second harmonic generation and three-wave-mixing processes are nonlinear optical effects based on the second order susceptibility of materials and are very effective in providing laser radiation over a wide range of wavelengths. However there is a sever limitation in a medium excludes the possibility of second order optical nonlinearity. One way to overcome this is the incorporation of suitable defects into the medium so as to avoid inversion symmetry [1–4].

We attempt to evaluate theoretically the second order optical nonlinearity in crystals of KCl:Li due to F_A color centers. The F_A center is considered as a three level system with the value of transition frequencies and dipole moments available from linear optical spectroscopy. The

¹E-mail address: majlesara@gmail.com, ara@msrt.it

non-vanishing ground state electrical dipole moment present in the system due to the difference in electro-negativities of the host and dopant cations is estimated. The density matrix formalism is employed and the equation of motion are solved by second order perturbation to evaluate the nonlinear optical susceptibility for second harmonic generation as well as frequency mixing. The spectral response of the real and imaginary parts of second order optical susceptibility is obtained and found to have reasonably large nonlinear response.

A Kramers-Kronig analysis is performed to study the effect of the color center on the dispersion of refractive index of the host crystal and the anomalous dispersion near resonance is explored as a method of phase matching. Frequency regions are identified where second order optical nonlinearity in these crystals can be used.

Our current interest is in the calculation of second order optical susceptibility that determines three wave mixing. The availability of materials for three-wave mixing is severely limited by the requirement of lack of inversion symmetry [5]. This has led to several attempts of overcoming the limitation. For example, application of a static electric field removes the inversion symmetry and molecular engineering of organic materials is used to design materials possessing the required asymmetry. We have recently suggested centro-symmetric containing point defects such as the F_A centers as an alternative class of a new second order medium [6]. The F_A center has an electron bound to a vacant anion site in the crystal with one of the neighboring cation sites occupied by a small monovalent impurity cation. By virtue of this structure, it does not basically have inversion symmetry and is capable of giving second order optical nonlinear response. The defect has the crystallographic orientation $\langle 100 \rangle$.

Produced by any coloration process, these color center are normally oriented by any coloration process, these color center are normally oriented at random in all the six $\langle 100 \rangle$ orientation. However, it is possible to align them preferentially along any one of the specific direction, say [001] and using polarized light [7]. If a [100] face of a crystal containing the F_A centers is irradiated with light of wavelength 556 nm and polarized in $\langle 100 \rangle$ direction and propagating in the [100] direction, most of the center will be aligned along the [100] direction. As a consequence, the nonlinearity does not get averaged out macroscopically, rendering the crystals useful for second order optical applications.

Theoretical studies on degenerate four wave mixing on crystals containing F , F_A , F_2^+ centers [8–13] and experimental studies on F_3^+ centers have shown that their third order optical center system in suitable host-impurity combination can be used to realize third harmonic generation and second harmonic generation [6] with reasonable efficiency. Since these centers are known to be laser-active, their optical nonlinearity hold special interest.

1.1 Model

An F center is modeled as an electron trapped in an anion vacancy. An F_A center is modeled as an F center with one impurity cation (L_i^+ in KCl: Li) as its nearest neighbour (NN). Model for the F_A center are given in Figure 1. The F center will be described by a four-level depicted described the fundamental absorption and associated down-shifted emission. In the present study, other higher excited states are not included. Electronic ground states for F and F_A centers are taken to be s -like. The first excited state in the case of the highly symmetric F center is taken to be p -like with three-fold degeneracy. For the F_A center the reduction in symmetry from the cubic F center to the tetragonal F_A center cause a splitting of the three fold degenerate p -like state into

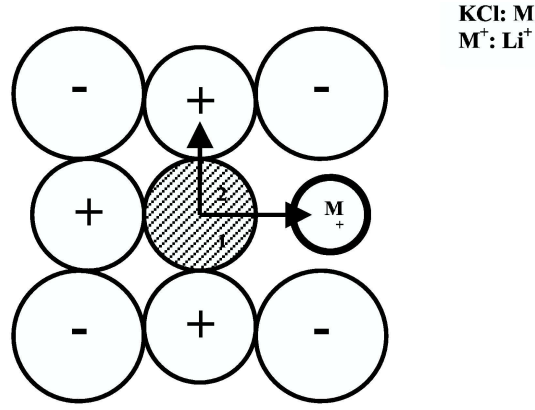


Fig. 1. Model for the F_A center. The dashed region denotes the F center and the associated nearest neighbor action impurity is marked M^+ . The A_1 and A_2 transition vectors are indicated by arrows along and perpendicular to the line joining the impurity and the center respectively.

two components-one transition polarized in the direction of the NN impurity cation (labeled F_{A1}) and a two-fold degenerate transition polarize in the plane perpendicular to it (labeled F_{A2} ; see Figure 2).

We take the following to be the general characteristics of the systems considered in this study.

- (a) The centers are stable at low temperatures against thermal and photo-thermal ionization.
- (b) Oscillator strengths for F_{A1} and each one of the two-fold F_{A2} transitions are equal irrespective of the energy splitting.
- (c) In the case of F_A centers the impurities are considered distributed equally among the six NNs. It is also possible to align these impurities by suitable thermo-optic treatment [8].

The second order susceptibility for a second harmonic generation three-wave mixing process $\chi^{(2)}(2\omega; \omega, \omega)$ relates the $P_{2\omega}$, the second order polarization at the second harmonic frequency to the interacting field by

$$P_{2\omega} = \text{Re}[E_\omega \cdot \chi^{(2)}(-2\omega; \omega, \omega) \cdot E_\omega], \quad (1)$$

$$E_\omega = A_{0\omega}(r)u_\omega \exp[i(\omega t - k \cdot r)], \quad (2)$$

where $A_i(r)$ are the position (r)-dependent amplitudes of the electric fields, u are unit vectors in the directions of these fields and k denote their wave vectors. The density matrix approach of treating the nonlinear polarization to second order in electric fields [13] leads to the expression for the second order susceptibility:

$$\begin{aligned} \chi^2(-2\omega, \omega, \omega) = & \frac{N}{2\eta^2} \left[\sum_{n,m,\nu} \frac{(\rho_m^0 - \rho_{\nu\nu}^0)}{(\omega + \omega_{n\nu} + i\Gamma_{nm})(2\omega + \omega_{nm} + i\Gamma_{nm})} \right. \\ & \left. + \frac{(\rho_{mm}^0 - \rho_{\nu\nu}^0)}{(\omega + \omega_{\nu m} + i\Gamma_{\nu m})(2\omega + \omega_{nm} + i\Gamma_{nm})} \right] \mu_{\nu m} \cdot \mu_{mn} \cdot \mu_{\nu\nu}, \quad (3) \end{aligned}$$

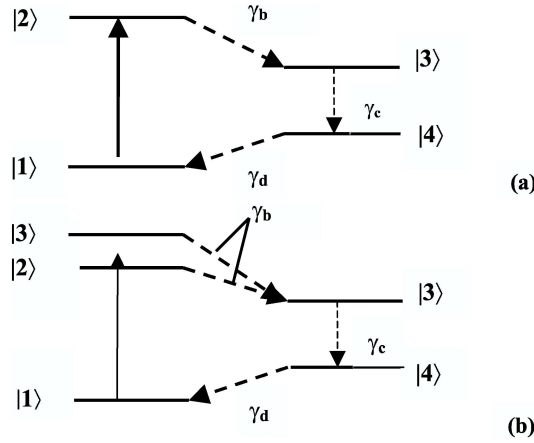


Fig. 2. The level schemes for (a) F center and (b) F_A center. Relaxation pathways are denoted by dashed arrow lines. γ_b, γ_d denote non-radiative relaxation rates. γ_c is the sum of radiative and non-radiative relaxation rates. In (b) levels $|2\rangle$ and $|3\rangle$ have the same relaxation rate γ_b .

where N is the density of oriented F_A centers, ρ_{ii}^0 are the elements of the unperturbed density matrix and $\hbar\omega_{kl}$ denotes the energy difference between levels k and l . The phenomenological damping coefficients corresponding to the transition from level k to level l is Γ_{kl} , μ_{kl} is the electric dipole moment of the transition k to l and \hbar is $(h/2\pi)$ where h is the Planck's constant. The input parameters are taken from published data [6,7]. The above equation for a 3-level system gives 27 individual terms each for the real and the imaginary parts. The initial conditions are $\rho_{nm} = \delta_{nm}$ with $\rho_{nm} = 0$ for $n > 1$. It is to be noted that the F_A center possesses a permanent electric dipole moment on two accounts the off-center site of the lithium ion gives rise to a static ionic displacement dipole moment. On the other hand, the lowered symmetry causes asymmetry of the electronic charge distribution on the impurity ion giving it another dipole moment of an electronic nature. Both are significant and it is the latter moment which is used for the present calculation to represent μ_{11} since we are concerned here with an optical response. In any case, the numerical magnitudes of the susceptibility scale linearly with this dipole moment without affecting the spectral variation. The influence of the coupling moments μ_{23} and μ_{32} is neglected. The transition frequencies are so defined such that $\omega_{mn} = \omega_{nm}$. Under these condition, several terms of Eq. 3 vanish and the contributions to the real part of susceptibility arise only from the six terms given below.

The susceptibility expression given below represents the effective scalar susceptibility and do not correspond to any specific tensor component. To get there latter components is easy but we prefer to deal with this effective susceptibility for convenience.

$$\chi_{Re}^{(2)}(-2\omega, \omega, \omega) = \frac{N}{2\eta^2} \left\{ \left[\frac{\omega + \omega_{12}}{(\omega + \omega_{12})^2 + \Gamma_{12}^2} + \frac{\omega - \omega_{12}}{(\omega - \omega_{12})^2 + \Gamma_{21}^2} \right] \frac{\mu_{21}\mu_{11}\mu_{12}}{2\omega} \right. \quad (4)$$

$$\left. + \left[\frac{\omega + \omega_{13}}{(\omega + \omega_{13})^2 + \Gamma_{13}^2} + \frac{\omega - \omega_{13}}{(\omega - \omega_{13})^2 + \Gamma_{31}^2} \right] \frac{\mu_{31}\mu_{11}\mu_{13}}{2\omega} \right.$$

$$\begin{aligned}
& + \left[\frac{-(\omega + \omega_{12}) \cdot (2\omega + \omega_{12}) - \Gamma_{12}\Gamma_{12}}{[(\omega + \omega_{12})(2\omega + \omega_{12}) - \Gamma_{12}\Gamma_{12}]^2 + [(\omega + \omega_{12})\Gamma_{12} + (2\omega + \omega_{12})\Gamma_{12}]^2} \right] \mu_{21}\mu_{11}\mu_{12} \\
& + \left[\frac{-(\omega + \omega_{13}) \cdot (2\omega + \omega_{13}) - \Gamma_{13}\Gamma_{13}}{[(\omega + \omega_{13})(2\omega + \omega_{13}) - \Gamma_{13}\Gamma_{13}]^2 + [(\omega + \omega_{13})\Gamma_{13} + (2\omega + \omega_{13})\Gamma_{13}]^2} \right] \mu_{13}\mu_{31}\mu_{11} \\
& + \left[\frac{-(\omega - \omega_{12}) \cdot (2\omega - \omega_{12}) - \Gamma_{21}\Gamma_{21}}{[(\omega - \omega_{12})(2\omega - \omega_{12}) - \Gamma_{21}\Gamma_{21}]^2 + [(\omega - \omega_{12})\Gamma_{21} + (2\omega - \omega_{12})\Gamma_{12}]^2} \right] \mu_{11}\mu_{12}\mu_{21} \\
& + \left. \left[\frac{-(\omega - \omega_{13}) \cdot (2\omega - \omega_{13}) - \Gamma_{31}\Gamma_{31}}{[(\omega - \omega_{13})(2\omega - \omega_{13}) - \Gamma_{31}\Gamma_{31}]^2 + [(\omega - \omega_{13})\Gamma_{31} + (2\omega - \omega_{13})\Gamma_{31}]^2} \right] \mu_{11}\mu_{13}\mu_{31} \right\}.
\end{aligned}$$

In a similar way the imaginary part is extracted and found to be given by

$$\begin{aligned}
\chi^2(2\omega, \omega, \omega) = \frac{-N}{2\eta^2} & \left\{ \left[\frac{\Gamma_{12}}{(\omega + \omega_{12})^2 + \Gamma_{12}^2} + \frac{\Gamma_{21}}{(\omega - \omega_{12})^2 + \Gamma_{21}^2} \right] \frac{\mu_{21}\mu_{11}\mu_{12}}{2\omega} \right. \\
& + \left[\frac{\Gamma_{13}}{(\omega + \omega_{13})^2 + \Gamma_{13}^2} + \frac{\Gamma_{31}}{(\omega - \omega_{13})^2 + \Gamma_{31}^2} \right] \frac{\mu_{31}\mu_{11}\mu_{13}}{2\omega} \\
& + \left[\frac{-(3\omega + 2\omega_{12})\Gamma_{12}}{[(\omega + \omega_{12})(2\omega + \omega_{12}) - \Gamma_{12}\Gamma_{12}]^2 + [(\omega + \omega_{12})\Gamma_{12} + (2\omega + \omega_{12})\Gamma_{12}]^2} \right] \mu_{12}\mu_{21}\mu_{11} \\
& + \left[\frac{-(3\omega + 2\omega_{13})\Gamma_{13}}{[(\omega + \omega_{13})(2\omega + \omega_{13}) - \Gamma_{13}\Gamma_{13}]^2 + [(\omega + \omega_{13})\Gamma_{13} + (2\omega + \omega_{13})\Gamma_{13}]^2} \right] \mu_{13}\mu_{31}\mu_{11} \\
& + \left[\frac{-(3\omega - 2\omega_{12})\Gamma_{21}}{[(\omega - \omega_{12})(2\omega - \omega_{12}) - \Gamma_{21}\Gamma_{21}]^2 + [(\omega - \omega_{12})\Gamma_{21} + (2\omega - \omega_{12})\Gamma_{12}]^2} \right] \mu_{12}\mu_{21}\mu_{11} \\
& + \left. \left[\frac{-(3\omega - 2\omega_{13})\Gamma_{31}}{[(\omega - \omega_{13})(2\omega - \omega_{13}) - \Gamma_{31}\Gamma_{31}]^2 + [(\omega - \omega_{13})\Gamma_{31} + (2\omega - \omega_{13})\Gamma_{31}]^2} \right] \mu_{11}\mu_{13}\mu_{31} \right\}.
\end{aligned} \tag{5}$$

2. Results and Analysis

Using the above equations, the real and imaginary parts of the second order susceptibility for second harmonic generation are evaluated as functions of ω values of Γ_{k1} are estimated from the half widths of optical absorption spectra. To assign a value for μ_{11} (the electronic part of the dipole moment on the lithium ion arising from asymmetry), we adopt the relation for the dipole moment (μ_{AB}) in Debye units that exists between two dissimilar atoms A and B with respective electro-negativities Ψ_A and Ψ_B given by [14]:

$$\mu_{AB} = \Psi_A - \Psi_B \tag{6}$$

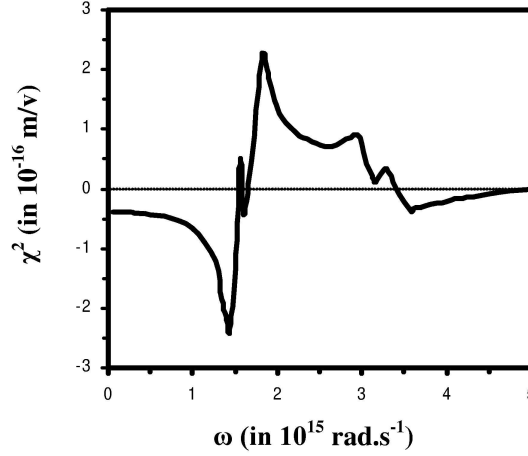
With the Pauling electro-negativities [8] of Li^+ and K^+ ions given by $\Psi_{Li} = 1.0$ and $\Psi_K = 0.8$, we get a value of 0.67×10^{-30} Cm for μ_{11} . The values of all the other input parameters are given in Table 1.

From the spectral response of the real part shown in Figure 3, we see that reasonably large magnitudes of the susceptibility are exhibited over a wide frequency region. The values of the susceptibility and the corresponding frequencies are shown in Table 2.

The frequency dependence of the imaginary part is depicted in Figure 4. Two well-defined peaks appear at $\omega = 3.0$ and 3.4×10^{15} rads^{-1} , which agree well with the transition frequency ω_{12} and ω_{13} of the system. Two negative peaks also appear at the angular frequencies 1.53 and

Tab. 1. Input parameters

$\omega_{12}(10^{15}\text{rads}^{-1})$	$\omega_{13}(10^{15}\text{rads}^{-1})$	$\Gamma_{12}(10^{13}\text{s}^{-1})$
3.008	3.418	9.09
$\Gamma_{13}(10^{14}\text{s}^{-1})$	$\mu_{12}(10^{-29}\text{Cm})$	$\mu_{13}(10^{-29}\text{Cm})$
1.44	1.2	1.6

Fig. 3. Real part $\chi^{(2)}(-2\omega; \omega, \omega)$ vs. ω .

$1.68 \times 10^{15} \text{ rads}^{-1}$, which are close to the subharmonics. It may also be noticed that the real part of the susceptibility shows a zero at a frequency where the imaginary part shows a peak.

2.1 Molecular hyperpolarizability

We begin this discussion by considering the expectation value of the dipole moment of the m th molecule, denoted by er_m , in terms of a power series in the electric field, similar to the series for the macroscopic polarization $P(t)$

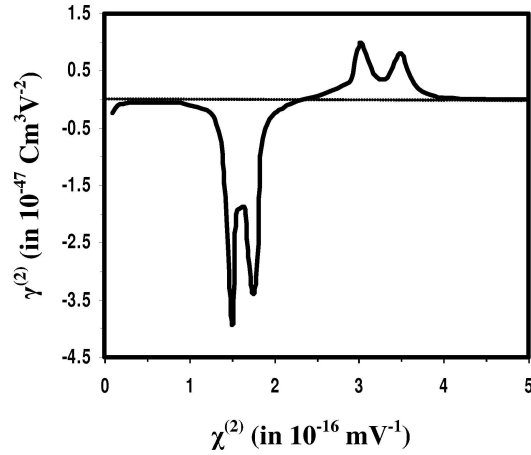
$$P(t) = N(er_m) \quad (7)$$

$$er_m = er_m^{(0)} + er_m^{(1)} + \dots + er_m^{(n)} + \dots \quad (8)$$

where $er_m^{(0)}$ is the permanent moment, $er_m^{(1)}$ is linear in the field, $er_m^{(2)}$ is quadratic, and so on. The term $er_m^{(0)}$ in the above expression represent the permanent electric dipole moment possessed by polar molecules. The various higher order terms ($n = 1, 2, \dots$) in the series can be related to

Tab. 2. Second order parameters of F_A center

ω	$1.56 \times 10^{15} \text{rads}^{-1}$	$1.76 \times 10^{15} \text{rads}^{-1}$
$\chi^{(2)}(-2\omega; \omega, \omega)$	$0.52 \times 10^{-19} \text{mV}^{-1}$	$2.30 \times 10^{-16} \text{mV}^{-1}$
$\gamma^{(2)}(-2\omega; \omega, \omega)$	$2.70 \times 10^{-50} \text{Cm}^3 \text{V}^{-2}$	$12.2 \times 10^{-50} \text{Cm}^3 \text{V}^{-2}$
ω	$2.90 \times 10^{15} \text{rads}^{-1}$	$3.30 \times 10^{15} \text{rads}^{-1}$
$\chi^{(2)}(-2\omega; \omega, \omega)$	$1.00 \times 10^{-19} \text{mV}^{-1}$	$0.35 \times 10^{-19} \text{mV}^{-1}$
$\gamma^{(2)}(-2\omega; \omega, \omega)$	$5.30 \times 10^{-50} \text{Cm}^3 \text{V}^{-2}$	$1.80 \times 10^{-50} \text{Cm}^3 \text{V}^{-2}$

Fig. 4. Imaginary part $\chi^{(2)}(-2\omega; \omega, \omega)$ vs. ω .

electric field $E_m(t)$ acting locally at the site of the m th molecule by:

$$P^{(n)}(t) = \frac{N}{n!} \int_{-\infty}^{\infty} d\omega_1 \dots \int_{-\infty}^{\infty} d\omega_n \gamma_m^{(n)}(-\omega, \omega_1, \dots, \omega_n) E_m(\omega_1) E_m(\omega_n) \exp(i\omega t) \quad (9)$$

where the Fourier components $E_m(\omega)$ related to the field $E_m(t)$ acting locally at the site of the site of the m th molecule by the transformation, and $\omega = (\omega_1 + \omega_2 + \dots + \omega_n)$ and γ_n is the molecular hyperpolarisabilities. On the other hand we know that:

$$P^{(n)}(t) = \varepsilon_0 \int_{-\infty}^{\infty} d\omega_1 \dots \int_{-\infty}^{\infty} d\omega_n \chi^{(n)}(-\omega, \omega_1, \dots, \omega_n) E(\omega_1) \dots E(\omega_n) \exp(i\omega t) \quad (10)$$

By comparison we can find a formula for the molecular hyperpolarisabilities [5]:

$$\gamma^{(2)}(-2\omega; \omega, \omega) = \frac{2\varepsilon_0 \chi^{(2)}(-2\omega; \omega, \omega)}{N f(\omega)} \quad (11)$$

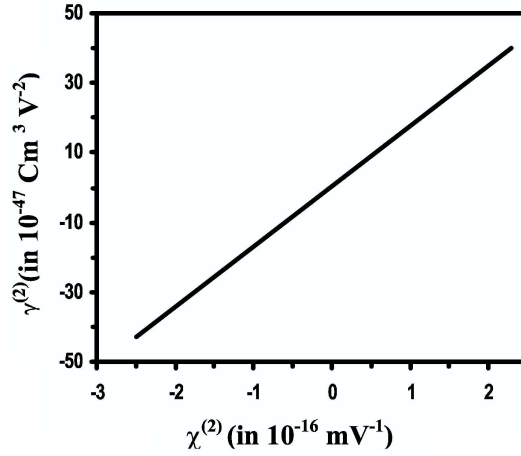


Fig. 5. Molecular hyperpolarisability as function of $\chi^{(2)}$.

where $f(\omega)$ is a local field factor estimates of the molecular polarizability for $f(\omega) = 1/3$ and substituting ϵ_0 and n we can calculate $\gamma^{(2)}$ as function of $\chi^{(2)}$ the result of such calculation is shown in Figure 5 and also is given in Table II. Evidently these values are larger than the molecular polarizability of *KDP* ($8.55 \times 10^{-53} \text{ Cm}^3 \text{ V}^{-2}$) calculated from its macroscopic susceptibility [16].

2.2 Phase matching

The practical realization of second harmonic generation depends on the coherence length given by:

$$l_c = \frac{\pi c}{\omega(n_\omega - n_{2\omega})} \quad (12)$$

where n_ω and $n_{2\omega}$ are refractive indices of the crystal at the crystal at the fundamental and second harmonic frequencies respectively, c is the speed of light in vacuum. The crystal containing color centers shows anomalous dispersion around the resonance region and this gives rise to the possibility of affording phase matching by a suitable choice of the operational frequencies. For instance, the refractive index of the host crystal (KCl) is known to increase with frequency [17]. The change in refractive index $\Delta n(\omega)$ due to the electronic absorption of F_A centers can be evaluated from the absorption spectrum using the Karamers-Kroning relation:

$$\Delta n(\omega) = (2/\pi)P \int_0^\infty \frac{\Omega k(\omega) d\Omega}{\Omega^2 - \omega^2} \quad (13)$$

where P indicates that the Cauchy principal value of the following integral is to be taken, $k(\omega)$ is the extinction coefficient at the frequency ω given by:

$$k(\omega) = \frac{c\alpha(\omega)}{2\omega} \quad (14)$$

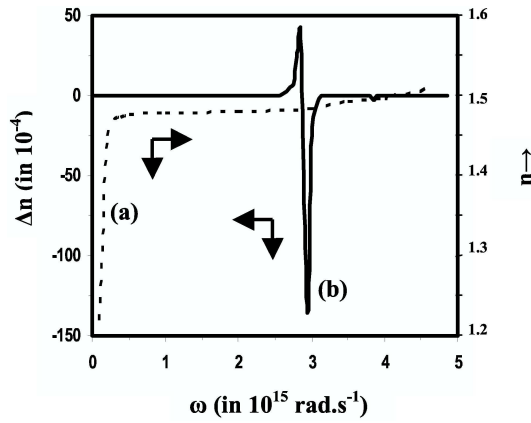


Fig. 6. (a) dashed line: refractive index n of KCl crystal vs ω (b) continuous line: Δn of F_A center in KCl:Li vs ω ($N = 1.2 \times 10^{23} m^{-3}$).

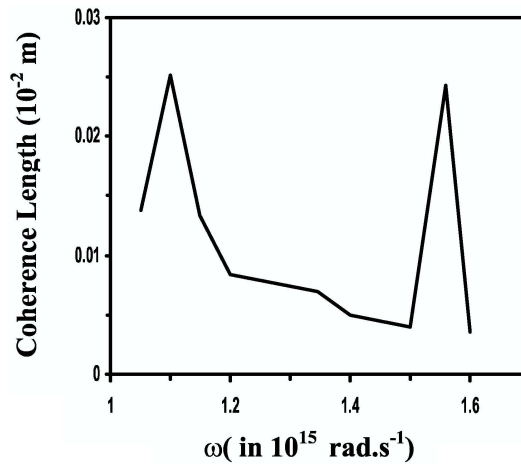


Fig. 7. Coherence length as a function of ω .

with $\alpha(\omega)$ representing the absorption coefficient.

The variation of the refractive index of the host crystal, viz., KCl as function of frequency is calculated. One may note that the refractive index remains close to 1.5 throughout the frequency range from $1.0 - 5 \times 10^{15} \text{ rad.s}^{-1}$ with a uniform rise towards the higher frequencies. Thus the refractive index of the host crystal at 2ω would be invariably larger than that at the fundamental frequency.

The change in the refractive index due to the defect center ($N = 1.2 \times 10^{23} m^{-3}$) is also calculated. The anomalous for the rise in refractive of the host near resonance by bringing closer

Tab. 3. Estimated value of coherence lengths for different choices of ω

$\omega(10^{15})\text{rad/s}$	n_ω	$2\omega(10^{15})\text{rad/s}$	$n_{2\omega}$	$\Delta n(10^{-4})$	$l_c(m \times 10^{-2})$
1.10	1.47482	2.20	1.48122	0	0.038
1.15	1.47483	2.30	1.48123	0	0.013
1.30	1.47485	2.60	1.48633	1.03632	6.21×10^{-3}
1.40	1.47487	2.80	1.48661	1.61982	5.75×10^{-3}
1.45	1.47488	2.90	1.48775	11.3900	4.6×10^{-3}
1.50	1.47492	3.00	1.49000	-120.000	0.020
1.55	1.47499	3.10	1.49043	-11.2600	4.25×10^{-3}
1.60	1.47589	3.20	1.49044	-3.3250	4.148×10^{-3}
1.65	1.47591	3.30	1.49210	-1.6300	3.57×10^{-3}
1.70	1.47800	3.40	1.49221	0	4.47×10^{-3}
1.75	1.47825	3.50	1.49360	-8.2000	0.016

the effective refractive index values at ω and 2ω there by making phase matching possible. Large values of coherence length l_c can be obtained by appropriately choosing 2ω in the resonance region. Table 3 gives the estimated value of coherence lengths for different choices of ω , the fundamental frequency. However, as 2ω in chosen near the optical absorption peak, there is considerable absorption of the generated second harmonic signals. Hence a judicious choice frequency has to be made such that the coherence length is reasonable and at the same time absorption is not too large.

3. Summary and Conclusion

Second order optical non-linearity due to F_A center in alkali halide crystals containing point defects is investigated for the first time. The density matrix formalism is employed in the calculation considering the F_A center as a three-level system with transition frequencies and dipole moments taken from optical spectroscopic data. The ground state dipole moment of F_A center due to the difference in electro-negativity of the host and dopant ions is estimated while the effect of the excited state dipole moment is not considered. A second order perturbative solution of the equation of the density matrix is used to evaluate the second order optical susceptibility. Real and imaginary parts of the susceptibility are separated and obtained as function of frequency.

The results clearly indicate that the F_A centers in KCl:Li have reasonably large optical non-linearity. For example, $\chi^{(2)}$ has a value $2.3 \times 10^{-16} \text{mv}^{-1}$ at a frequency $1.75 \times 10^{15} \text{ rad/s}$ in KCl:Li with a moderate F_A center concentration of 10^{-16}mv^{-1} . The ground state dipole moment value obtained from electro-negativity consideration is varied in order to ensure that the qualitative features of the present studies are unaffected by any inaccuracy in the value of the dipole moment. The dependence of $\chi^{(2)}$ on μ_{11} is found to be linear.

It is seen that phase matching is possible in the system using the anomalous dispersion of refractive index in colored crystal estimated by a Kramer-Kroing analysis. A large reduction in refractive index near resonance yields reasonably large values of coherence lengths for certain

frequencies. It is also important to see that the generated second harmonic is not being absorbed to a large extent by the medium itself. There exist frequency regions with large $\chi^{(2)}$ where reasonable coherence lengths can be realized without high re-absorption of the second harmonic. Since it has been experimentally demonstrated that ordered F_A center can actually be produced and handled, it appear that there is certainly scope for experimentally investigating these media as practical systems for second harmonic generation.

References

- [1] V. Valerii Ter-Mikirtychev: *Applied Optics* **37** (1998) 6442-6445.
- [2] T. Tsuboi: *Applied Physics B: Laser and Optics* **69** (1999) 81-83.
- [3] S. B. Mirov, V. V. Fedorov, L. Xie, B. Boczar, R. Frost, B. Pryor: *Optics Communications* **199** (2001) 201-205.
- [4] M. R. Maria; P. Massimo: *Optics Communications* **209** (2002) 201-208.
- [5] P. N. Butcher, D. Cotter: *The Elements of Nonlinear Optics*, Cambridge University Press, Cambridge 1990.
- [6] M. H. Majlesara, C. Vijayan, Y. V. S. M. Murity: *Non-linear Optics* **26** (2001) 313-323.
- [7] F. Luty: *Physics of Color Centers*, Chap. 3 Ed. W. B. Fowler Academic Press NY, 1986, p. 181-291.
- [8] C. V. Krishnamurti, Y. V. J. M. Murity: *Mol. Cryst. Liq. Crst. Science and Technol. B: Nonlinear Optics* **2** (1992) 337-346.
- [9] C. V. Krishnamurti, Y. V. J. M. Murity: *Mol. Cryst. Liq. Crst. Science and Technol. B: Nonlinear Optics* **4** (1993) 91-97.
- [10] C. L. Cesar, M. N. Islam, C. E. Soccolich, R. D. Feldman, R. F. Austin, K. R. German: *Optics Letters* **15** (1990) 1147-1149.
- [11] I. Schneider, M. J. Marrone: *Optics Letters* **4** (1979) 390-392.
- [12] D. Wandt, W. Gellermann, F. Luty, H. Welling: *Journal of Applied Physics* **61** (1987) 864-869.
- [13] D. Marcuse: *Engineering Quantum Electrodynamics*, Brace and World Inc; New York 1970.
- [14] P. W. Atkins: *Physical Chemistry*, ELSB Oxford University Press; London 1978.
- [15] L. Pauling: *Nature of Chemical Bond and Structure of Molecules and Crystals*, Ox and IBH, Calcutta 1960.
- [16] A. Yariv: *Quantum Electronics*, John Wiley, Singapore 1989.
- [17] P. G. Walter, W. Vaubhan: *Handbook of Optics*, McGraw-Hill Book 1978.